Snow Microwave Emission Modeling of Ice Lenses within the Snowpack Using the Microwave Emission Model for Layered Snowpacks (MEMLS)

B. MONTPETIT,[1] A. ROYER,[1] A. ROY,[1] A. LANGLOIS,[1] AND C. DERKSEN[2]

ABSTRACT

Ice lens formation, which follows rain on snow events or melt-refreeze cycles in winter and spring, is likely to become more frequent as a result of increasing mean winter temperatures at high latitudes. These ice lenses significantly affect the microwave scattering and emission properties and, hence, snow brightness temperatures that are widely used to monitor snow cover properties from space. To understand and interpret the spaceborne microwave signal, the modeling of these phenomena needs improvement. This paper shows the effects and sensitivity of ice lenses on simulated brightness temperatures using the Microwave Emission Model of Layered Snowpacks (MEMLS) coupled to a soil emission model at 19 and 37 GHz in both horizontal and vertical polarizations. Results when considering pure ice lenses show an improvement of 20.5 K of the root mean square error (RMSE) between the simulated and measured Tb using several in situ datasets acquired during field campaigns across Canada. The modeled brightness temperatures were found to be highly sensitive to the vertical location of ice lenses within the snowpack.

Keywords: ice lens, passive microwave, remote sensing, snow, snow modeling.

INTRODUCTION

With increasing mean winter temperatures in many regions of the northern hemisphere (Serreze and Barry, 2011; Ye et al., 2008), there have been observations of mid-winter melt-refreeze cycles (Bartsch et al., 2010; Stien et al., 2010) and more frequent winter rain events (Putkonen et al., 2011; Rennert et al., 2009). These events create ice lenses at the surface or within the snowpack through drainage (Rees et al., 2010). It is known that ice lens formation increases the mean soil temperature by releasing latent heat during the freezing process, and ice lenses create impermeable ice barrier layers. Ice lenses also reduce the mid-winter vegetation respiration and modify the physical properties of snow (Grenfell and Putkonen, 2008) due to the weak thermal diffusivity of ice. It has also been reported that the formation of ice lenses within the snowpack affects the feeding habits of ungulate species in northern regions (Hansen et al., 2011; Miller et al., 1975; Rennert et al., 2009; Serreze and Barry, 2011). Identifying the formation of ice lenses at the regional scale and monitoring their spatial extent requires further study.

Microwave remote sensing (both passive and active) has proven useful in the detection of ice lenses (Bartsch et al., 2010; Lemmetyinen et al., 2010; Rees et al., 2010). However, the coarse spatial resolution of the microwave signal is not only affected by ice lenses but also by other

[1] Centre d'Applications et de Recherches en Télédétection (CARTEL), Université de Sherbrooke, Sherbrooke, QC, Canada.
[2] Climate Research Division, Environment Canada, Toronto, ON, Canada.

contributions such as the snow properties, bare ground, vegetation, lake ice, as well as topographic and atmospheric effects (Mätzler, 2006). Microwave radiative transfer models are important tools for improving our understanding of the effects of the different environmental parameters on the measured signal (e.g., Grody, 2008; Langlois et al., 2011; Pulliainen et al., 1999; Wiesmann and Mätzler, 1999). In this study, we focus on analyzing ice lenses but acknowledge that large uncertainties remain, however, due to the parameterization of the snow grain size (Durand and Liu, 2012; Langlois et al., 2012; Roy et al., 2012).

Another uncertainty in these radiative transfer models is the soil contribution. Several studies have been conducted to model soil emissivity at lower frequencies (Prigent et al., 2000; Wigneron et al., 2011), but it is poorly documented for frequencies above 19 GHz. Wegmüller and Mätzler (1999) developed a soil emissivity model that is implemented in the HUT radiative transfer model based on 19 and 37 GHz measurements (Pulliainen et al., 1999). Since this soil model was derived from in situ measurements of bare soil, it has to be tested on different types of surfaces.

The main objective of this study is to simulate Tb using MEMLS for snowpacks with ice lenses using measured in situ properties of the ice lenses (depth, thickness, and temperature), assuming pure ice lenses, and determine the sensitivity of the ice lens parameters on the modelled Tb. Specifically, we want to a) optimize the characterization of the snow grain size and the soil roughness for snowpacks without ice lenses and b) validate the simulations with in situ Tb measurements acquired with ground-based radiometers during winter field campaigns across Canada to evaluate the performance of this modelling. Refer to Montpetit et al. (2012b) for more details on this current study.

DATA AND METHODS

Measurements from three field campaigns across Canada in Arctic, sub-Arctic, and mid-latitude regions were used in this study: 1) Daring Lake, Northwest Territories; 2) Churchill, Manitoba; and 3) south-eastern Québec (St-Romain and Sherbrooke). The first campaign was in April 2007 near Daring Lake (64° 50’ N, 111° 38’ W), Northwest Territories, Canada. Brightness temperatures (Tb) using a sled-based passive microwave radiometer system (6.9, 19, 37, and 89 GHz) were measured at 8 undisturbed sites. Measurements were also made after removing a surface ice lens created by a rain-on-snow event in late winter. A complete description of the measurements is found in Rees et al. (2010). Figure 1 shows the locations of all the studied sites.

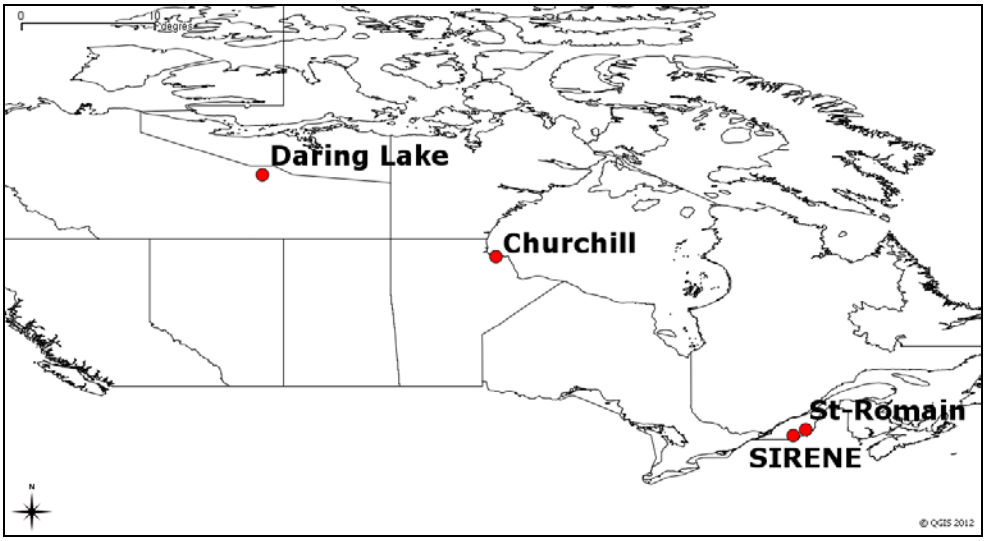

Figure1. A map of Canada showing the location of all the studied sites for this research.

At the second site, Tb (using the same sled-based radiometer system) and detailed snowpit physical properties were taken in forest clearings near Churchill (58°46' N, 94° 11' W), Manitoba, at regular intervals during the 2009–2010 winter season as described in Derksen et al. (2012). During measurement periods in March and April, ice lenses that were the result of melt-refreeze events were observed and measured in the snowpack.

During the winter of 2011, similar Tb and snowpit measurements were taken at two different sites in southeastern Québec, Canada. The first site was an open grassy area located in the town of St-Romain (45° 47' N, 71° 1' W) where thick ice lenses (1 to 2 cm) were observed within the snowpack after a prolonged melt-refreeze event in February 2011. The second site was located at the *Site Interdisciplinaire de Recherche en ENvironnement Extérieur* (SIRENE), a research station of the *Centre d'Applications et de Recherches en TELédétection* (CARTEL), on the Université de Sherbrooke main campus (45° 22' N, 71° 55' W). This site is also an open grassy area, but the ice lenses were created artificially by gently spraying water on top of the snowpack on cold days (< −15°C). This created a thin ice lens at the surface of the snowpack because the water froze immediately on contact with snow. The gentle spray created a smooth ice surface. When the first artificial lens was buried by subsequent snowfall, a second surface ice lens was created by spraying the area once more.

In situ data

To properly optimize the snow grain size parameter and the soil roughness parameter for the microwave radiative transfer model (MEMLS), sites without ice lenses were chosen. Afterwards, to test the ice lens treatment with a modified version of MEMLS (see below), sites with ice lenses within the snowpack were chosen.

For the Daring Lake campaign in 2007, the grain size measurements were made manually using a gridded reference card and a field microscope (D_{max}). The p_c were then derived from these measurements using the non-linear method of Durand et al. (2008). The measurements were taken in a tundra environment.

Brightness temperature data

Tb measurements were acquired using surface-based radiometers (SBR) on mobile sleds at an incidence angle of 55°. Calibrations were conducted on a regular basis using warm (ambient temperature microwave absorber) and cold (liquid nitrogen) targets as described by Asmus and Grant (1999) and Solheim (1993). Uncertainty in the measurement of the calibration target temperature was estimated at ± 2 K. The 19 and 37 GHz radiometers were calibrated simultaneously so that the same target temperature uncertainties for a given calibration applied to both frequencies. Radiometer stability depended on the frequency and varied somewhat from campaign to campaign, but the overall precision was estimated at ± 2 K at 19 GHz, and < 1 K at 37 GHz, based on a 3-db width of the main beam.

Models

The passive microwave snow radiative transfer model used in this study was the Microwave Emission Model of Layered Snowpacks (MEMLS) (Wiesmann and Mätzler, 1999). This model was used because of its multi-layer design which enabled discrete ice lens treatment for pure ice layers within the snowpack. Moreover, we added a soil model (Wegmüller and Mätzler, 1999) to improve the estimation of the soil contribution under the snow.

Snow emission model

The MEMLS snow emission model describes the snow cover as a stack of horizontal layers characterized by the snow's temperature, density, thickness, liquid water content, salinity, and grain size. The radiative transfer parameters (reflection and refraction at layer interfaces and layer reflection and absorption) are based on physical equations integrated in a six-flux stream parameterization. A combination of coherent and incoherent superposition is used to calculate the signal transmission between every layer interface (see Mätzler and Wismann, 1999, and Wismann and Mätzler, 1999, for a complete description of the model). In this study, the scattering

coefficient of each snow layer was determined by the improved Born approximation (Mätzler, 1998a).

Durand et al. (2009) showed that the most sensitive parameter in MEMLS is the snow grain size. The snow grain size parameter used in MEMLS is the correlation length (p_c). According to Debye et al. (1957) and Mätzler (2002), this parameter is related to the snow grain optical diameter (D_o) by the following relationship:

$$p_c = \frac{2}{3} D_o (1 - \nu) \tag{1}$$

where ν is the ice fraction (ρ_{snow} / ρ_{ice}). D_o was derived from measurements of the specific surface area of snow grains (SSA): $D_o = \frac{6}{\rho_{ice} SSA}$. The SSA parameter can be accurately measured in the field by shortwave infrared reflectometry (e.g., Montpetit et al., 2012a). Another way to define p_c is to use the longest diameter of the snow grain (D_{max}; Fierz et al., 2009). Durand et al. (2008) derived the following relationship between p_c and D_{max}:

$$p_c = \begin{cases} 0.18 + 0.09 \ln D_{\max} \pm 0.03 & \text{for } \rho_{snow}/\rho_{ice} > 0.2 \text{ and } D_{\max} > 0.125 mm \\ 0.05 \pm 0.015 & \text{otherwise} \end{cases} \tag{2}$$

However, recent studies (Brucker et al., 2011; Roy et al., 2012) show that the SSA needs to be calibrated for microwave radiative transfer models as previously discussed by Mätzler (2002) and Wiesmann et al. (2000). These studies, however, used different snow emission models or did not use SSA measurements for the snow grain size parameterization. Hence, it is necessary to validate the need for this correction factor. A method similar to Brucker et al. (2011) and Roy et al. (2012) was used in this study to estimate the correction factor. Here, the correlation length was adjusted with a multiplying factor ϕ to minimize the root mean square error (RMSE) between the measured and simulated Tb using MEMLS at 37 GHz.

$$p_c' = \phi p_c \tag{3}$$

Among the sites without ice lenses, only those for which the soil did not affect the Tb at 37 GHz (11 sites) were chosen (the selection was made by a sensitivity study using the measured snowpack characteristics; see Roy et al., 2012). This ensured that the correction factor ϕ addressed the errors due to the snow grain size parameterization and not errors in the soil modeling. Moreover, since the penetration depth of the microwave signal at 37 GHz is lower than at 19 GHz, this channel makes it less sensitive to the soil emissivity.

Ice lens modelling

In this study, ice lenses are characterized by their temperature, vertical position in the snowpack, and thickness. To simulate an ice lens with no scattering using IBA of MEMLS, the density of the ice lenses was considered constant in this study (density of pure ice = 917 kg m^{-3}). This renders the scattering coefficient null given by equation 25 of Mätzler (1998b). The ice lens model of Grody (2008) was also implemented in MEMLS. With this model, the ice lenses were associated with a non-scattering type (scattering coefficient was null) with attenuation described below. The dielectric constant of the ice layers was calculated using the equations of Mätzler (1998b) for pure

ice. The layer interface reflectivity values were calculated using the Fresnel equations. The ice lens model was defined by the absorption coefficient (α_{ice}) and the ice transmissivity (τ_{ice}), and it was calculated using the equations of Grody (2008):

$$\alpha_{ice} = \frac{2\pi}{\lambda}\frac{\varepsilon''}{\sqrt{\varepsilon'}} \tag{4}$$

$$\tau_{ice} = \exp(-\alpha_{ice} d_{ice} \sec\theta) \tag{5}$$

where ε' and ε'' are respectively the real and imaginary parts of the pure ice dielectric constant, d_{ice} is the ice lens thickness (in cm), and θ is the propagation angle within the ice lens. Finally, the ice emitted Tb was calculated as follows:

$$Tb_{ice} = (1-\tau_{ice})T_{ice} \tag{6}$$

where T_{ice} is the ice physical temperature (K).

Soil model

The soil reflectivity model proposed by Wegmüller and Mätzler (1999) determines the soil interface reflectivity, at a given frequency, in horizontal polarization (Γ_H) and vertical polarization (Γ_V) with the following equations for an incidence angle lower than 60°:

$$\Gamma_H = \Gamma_H^{Fresnel} \exp(-(k\sigma)^{\sqrt{-0.1\cos\theta}}) \tag{7}$$

$$\Gamma_V = \Gamma_H \cos\theta^{\beta} \tag{8}$$

where k is the wave number, σ is the soil roughness parameter, θ is the incidence angle, and β is a factor which was set to 0.655 by Wegmüller and Mätzler (1999). Here, we consider σ and β as two unknowns to be determined.

In this study, σ and β were determined by minimizing the biases between the modeled and measured Tb using MEMLS at 19 GHz V-Pol (19V) and H-Pol (19H) and different values of soil reflectivity for both polarizations. Only sites where snow had a minimal impact were chosen (9 sites). With this derived optimal reflectivity and the known incidence angle, β was determined from (8) as the following:

$$\beta = \log\left(\frac{\Gamma_V}{\Gamma_H}\right) \Big/ \log(\cos\theta) \tag{9}$$

Having obtained this factor, the roughness parameter for both frequencies was determined by minimizing the RMSE between the optimal and modeled reflectivity at 19 GHz using MEMLS with (7).

ICE LENS MODELING VALIDATION

Prior to the ice lens modelling analysis, the snow and soil parameterizations were optimized for snowpits without ice lenses and snowpits where ice lenses were removed. This allowed us to minimize the snow model uncertainties, assuming that the snow properties remained similar for

the corresponding snowpits with ice lenses. Afterwards, an analysis and validation of the ice lens treatment was conducted on two independent datasets.

Snow and soil optimizations

Based on the method described in the previous section, Tb simulations were performed at 37 GHz using MEMLS with values of factor ϕ ranging from 0 to 3 with an increment of 0.1 for 11 selected sites where the contribution of the soil was deemed to be negligible as discussed by Roy et al. (2012) Those sites, without ice lenses, where selected because the brightness temperature only depended upon the snowpack characteristics (mainly grain size), ensuring that ϕ was not biased by hypotheses concerning the soil conditions. Those sites showed a weak variation lower than 5 K for the modelled Tb for soil reflectivity ranging from 0 to 0.5 (range measured by Wegmüller and Mätzler, 1999). The RMSE ϕ (subscript ϕ is to differentiate the RMSE of the grain size optimization from the other RMSE) was then calculated with the measured Tb:

$$RMSE_{\phi} = \sqrt{\frac{\sum_{i=1}^{N}\left[(Tb_{sim;i}^{37V} - Tb_{mes;i}^{37V})^2 + (Tb_{sim;i}^{37H} - Tb_{mes;i}^{37H})^2\right]}{2N}} \quad (10)$$

where $Tb_{sim;i}$ and $Tb_{mes;i}$ are respectively the simulated and measured brightness temperatures for the sites "*i*" and *N* is the total number of sites used for the snow grain size optimization. Figure 1 shows the relationship between the calculated RMSE ϕ and the correction factor ϕ applied to the snow grain size for each simulation. The range of correction factor presented in Figure 2 was chosen to make sure the minimum RMSE ϕ found was not only a local minimum. This shows strong sensitivity to the snow grain size over the range of ϕ values; the RMSE ϕ is 17.6 K for no correction (ϕ = 1) and 13.7 K for the best fit obtained with ϕ =1.3 (Figure 1). While there is a need to evaluate this factor in future studies using larger datasets and the known uncertainties of the snow grain size measurements, this factor was applied to all the simulations in this study.

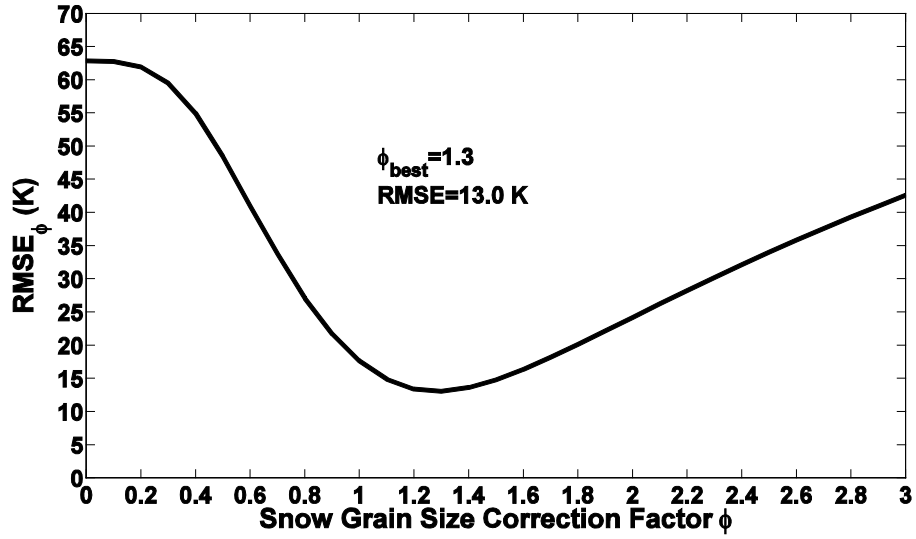

Figure 2. Snow grain size optimization at 37 GHz using MEMLS (root mean square error between measured and simulated Tb for selected sites without ice lenses or a soil contribution.

The next step in optimizing the simulation was to determine the best β factor (soil contribution) in (9) using the method described in the previous section. Using the correction factor ϕ in the Tb simulations, the optimal reflectivity values were determined by minimizing the biases between the

simulated and measured Tb for both polarizations (V and H) at 19 GHz. The results of these optimizations and the reflectivity ratios (Γ_V/Γ_H) for the polarizations and for 20 sites are available upon request. There are important variations in the derived ratio values. This is possibly due to the fact that the residual error introduced by the snow grain size variations between the sites remained important. Considering only the sites where the snow grain size had little influence on the modeled Tb, the mean ratio is 0.40 ± 0.23, $\beta = 1.72$.

Using (7) and (8) and the β factor calculated previously, the soil reflectivity was calculated by iterations on the soil roughness parameter. Two types of sites were distinguished: 1) mid-latitude grassy sites (referred to as "grass") and 2) tundra sites ("tundra"). The optimal soil roughness parameters for these two types of sites were determined by minimizing the RMSE ($RMSE_\sigma$) between the optimal soil reflectivity and the modeled reflectivity:

$$RMSE_\sigma = \sqrt{\frac{\sum_{i=1}^{N}\left[(\Gamma'_V - \Gamma_V)^2 + (\Gamma'_H - \Gamma_H)^2\right]}{2N}} \tag{11}$$

Figure 3 shows the relationship between the $RMSE_\sigma$ and the soil roughness parameters. The optimal parameters were found to be $\sigma_{grass} = 1.1$ cm (RMSE$\sigma = 0.04$) for the grass sites and $\sigma_{tundra} = 0.4$ cm (RMSE$\sigma = 0.07$) for the tundra sites.

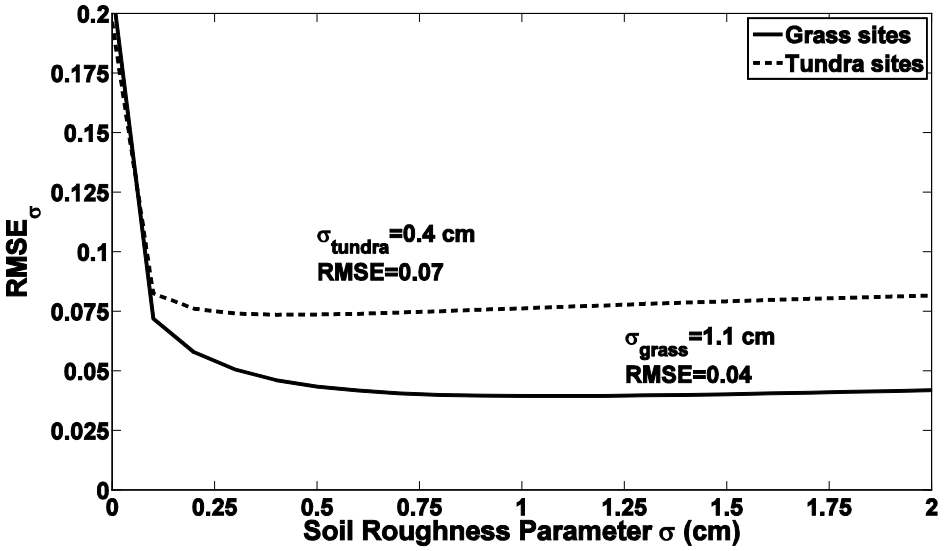

Figure 3. Optimization of the soil roughness parameter using the soil model of Wegmüller and Mätzler (1999) at 19 GHz for the grass sites (solid line) and the tundra sites (dashed line).

The results for the snow simulations at 19 and 37 GHz and V and H polarizations were then determined using $\phi = 1.3$, $\beta = 1.72$, σ_{grass}, and σ_{tundra} for all the sites without ice lenses, including the sites not considered in the optimization process. Figure 4 shows the comparison between the measured and modeled Tb (top left), the comparison between the H and V polarizations at 19 GHz (top right), the comparison between the H and V polarizations at 37 GHz (bottom left), and the comparison between the 19 and 37 GHz frequencies in V polarization.

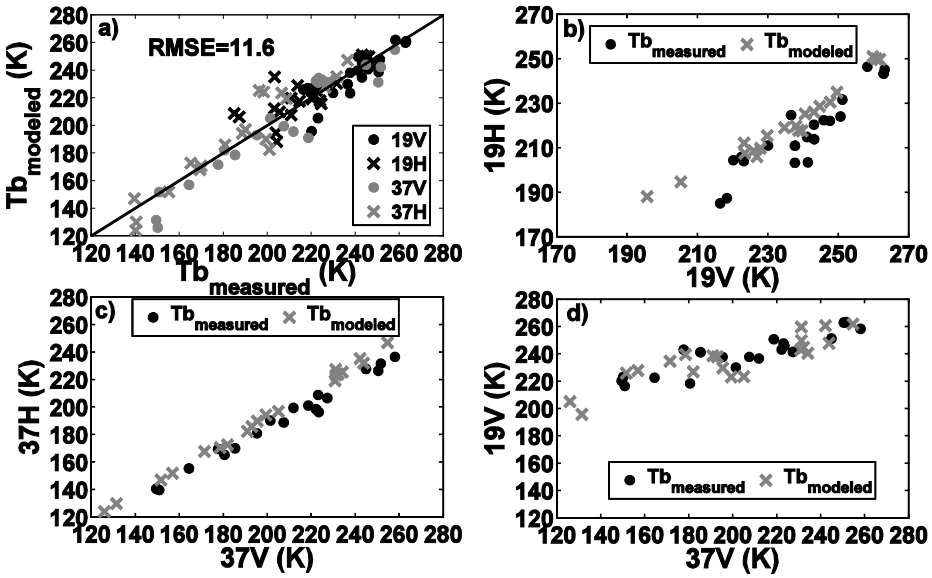

Figure 4. MEMLS simulations with φ = 1.3 and optimized σ for all 20 snowpits without ice lenses for 19 and 37 GHz and two polarizations H and V. (a) modeled Tb compared to measured Tb, overall RMSE is shown; (b) Tb at 19H vs. Tb at 19V; (c) Tb at 37H vs. Tb at 37V; (d) Tb at 19V vs. Tb at 37V.

The cross-polarization figures show that the soil contribution was adequately taken into account in the modeled Tb since the modeled and measured Tb are significantly correlated. The scatter in Figure 3b at 19 GHz comes from variability in the soil reflectivity. The correlation at 37 GHz, where the soil contribution is less important, is better than at 19 GHz. The modeled spectral dependency (19V vs. 37V) is also well correlated with the measured spectral dependency. This shows that using the same correction factor for the snow grain size for both frequencies is adequate. The overall RMSE between the modeled and measured Tb is 11.6 K, which is comparable to similar published results (Brucker et al., 2010; Lemmetyinen et al., 2010; Roy et al., 2012). Table 1 gives the RMSE for the four different channels (19V, 19H, 37V, and 37H) presented in figure 4. The higher errors in H-Pol could be explained by the increased sensitivity to stratigraphic variability (i.e., density). The lower errors at 19 GHz can be explained by the lower sensitivity to the snow grain size.

Since the snowpack conditions at the sites without ice lenses were similar to those with ice lenses, the optimal parameters (ϕ = 1.3, β = 1.72, σ_{grass}, and σ_{tundra}) previously derived were also applied to those sites. The next section analyzes the MEMLS simulations including the ice lens model.

Analysis of the snow and ice emission model

To evaluate the performance of the ice lens treatment described in the previous section, a preliminary simulation for all 6 sites with ice lenses was performed without a specific treatment for the ice lenses. Figure 5a shows the comparison between the measured Tb and the modeled Tb without the ice lens treatment at 19 and 37 GHz and V and H polarizations. The overall RMSE between the modeled and measured Tb is 34.5 K, mainly due to the Tb values at H polarization. As expected, the RMSE is significantly higher than was determined for snowpacks without ice lenses (RMSE = 11.6 K, see Figure 4), meaning that the error is attributable to the presence of an ice lens.

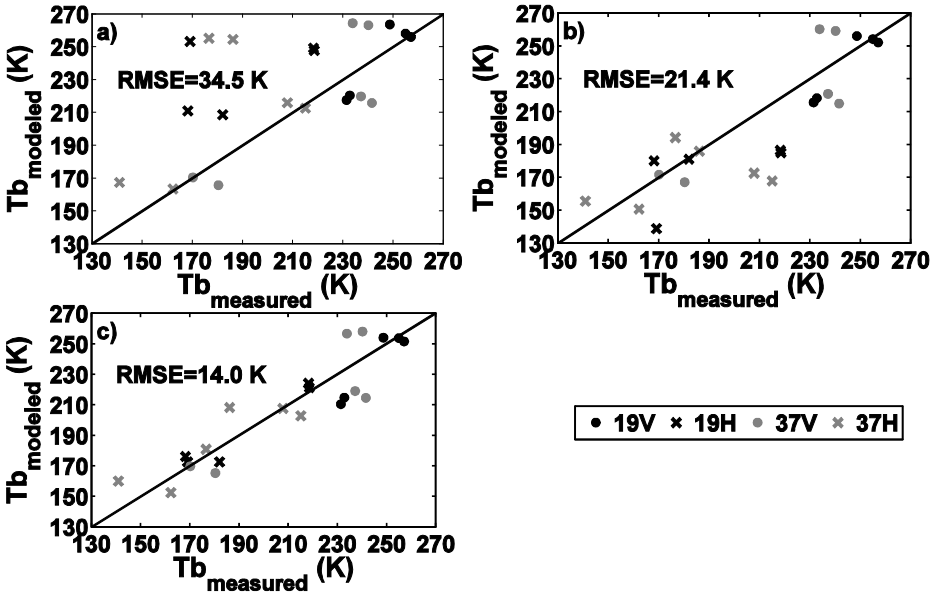

Figure 5. MEMLS was used to model Tb without an ice lens (a), with an ice lens at the surface of the snowpack (b), and with ice lenses at their measured depths within the snowpack (c), with φ = 1.3 and optimized σ compared to measured Tb for all 6 sites having ice lenses for 19 and 37 GHz and two polarizations H and V. Overall RMSE are shown for each case.

Grody (2008), Lemmetyinen et al. (2010), and Rees et al. (2010) modeled the effects of ice lenses on top of a snowpack. Figure 5b shows a comparison of the measured and modeled Tb when the ice lens was arbitrarily simulated at the top of the snowpack. The overall RMSE (21.4 K) shows an improvement of 13.1 K (38%) when compared to the simulations without the ice lens treatment (Figure 5b compared to Figure 5a). However, the RMSE in Figure 5b still remains higher than the mean level of error for snowpacks without an ice lens (Figure 2). This shows that the vertical position of the ice lenses within the snowpack must be taken into account.

Figure 5c shows the results with the ice lenses modeled at their measured depth within the snowpack. Again, an improvement of 7.4 K (35%) in the RMSE (14.0 K) is observed relative to the results of Figure 5b, and an improvement of 20.5 K (59%) is achieved compared to the results of Figure 5a. This shows the importance of modeling ice lenses at their exact depths within the snowpack. Also, the RMSE of Figure 5c is comparable to the RMSE presented in Figure 4 (11.6 K) for snowpacks where no ice lenses were present. This indicates that the error in Figure 5c most likely comes from the snow modeling rather than the ice lens treatment. Table 1 summarizes the RMSE between the modeled and measured Tb for all four channels presented in Figures 4 and 5.

Table 1. RMSE between the modeled and measured Tb for four channels for the sites with ice lenses compared to the reference sites without ice lens.

	RMSE (K)				
	No ice	Without ice lens	Ice lens on top	Ice lens within	Ice lens within
Channel	Figure 5	Figure 7a	Figure 7b	Figure 7c	Grody [18] equations
19V	9.4	10.8	10.4	12.9	12.4
19H	12.1	47.7	25.3	6.9	13.0
37V	12.1	21.0	19.2	18.8	18.0
37H	12.4	43.9	26.3	13.6	12.5
All	11.6	34.5	21.4	14.0	14.3

The ice lenses do not seem to affect the Tb in V-Pol at either frequency (standard deviation of 1.5 K at 19V and 3.9 K at 37V between the results of Figure 4 and 5). The greatest impact of the ice lenses can be seen in H-Pol. It is known that H-Pol is more sensitive to snowpack stratigraphy. This explains the major improvement in H-Pol at both frequencies that is achieved by the addition of a proper ice lens parameterization in MEMLS. Table 1 also gives the results of the ice lens modeling using the equations of Grody (2008). The differences between both parameterizations are mainly given by the absorption coefficient calculation which slightly differ (Grody, 2008; Mätzler, 1998b). Nonetheless, it is fair to say that the IBA theory is valid with a difference of 0.3 K in the overall RMSE.

Ice lens modeling at Daring Lake

To further validate the ice lens model presented in this study, the same analysis was conducted on another independent dataset provided by Rees et al. (2010). However, the major difference between the analyses of this dataset is the snow grain size measurements. It was thus necessary to determine another correction factor ϕ to optimize the simulations.

The same optimization process was conducted to minimize the errors due to the snow grain size and soil roughness. To do so, three sites (sites 5, 6, and 7 of Rees et al. [2010]) were selected. These sites were selected because the snowpack under the ice lens was sufficiently thick to minimize any soil effects at 37 GHz. The results of the snow grain size optimization at 37 GHz showed no need for correction ($\phi = 1$) meaning that the parameter D_{max} without correction gives the minimum $RMSE_{\phi} = 19.3$ K. The soil roughness parameter at 19 GHz for all the sites (the sites were all measured in the same region) was found to be $\sigma = 0.0$ cm (minimum $RMSE_{\sigma} = 0.097$). The fact that the soil roughness parameter is null suggests that the soil roughness had a minimal effect on reflectivity at 19 GHz. Also, the best parameter derived for the soil reflectivity ratio was $\beta = 2.50$.

Figure 6 shows comparisons between the modeled and measured Tb at 19 and 37 GHz and V and H polarizations for a) the layers of snow under the ice lenses (i.e., without ice lenses), b) simulations without ice lenses, and c) with the ice lenses modeled at their measured depths. The simulations in Figure 6a were conducted to determine the errors coming from the snow simulation (RMSE = 19.8 K). This RMSE (19.8 K) is comparable to the RMSE of the simulations with the ice lenses at their exact depths (15.9 K). This is a good indicator that the residual error in Figure 6c is more likely due to the snow modeling rather than the ice lens modeling. Also, the RMSE shows an improvement of 19.6 K with the ice lenses compared to simulations without ice lenses. The fact that the 19H and 37H channels led to greater overestimates may indicate that the snow grain size parameter did not adequately simulate snow scattering.

The results for the sites at Daring Lake, characterized by the geometrical diameter (D_{max}), appear to be less accurate than the previous sites, characterized by the optical diameter (D_{opt}). In fact, the accuracy of the D_{opt} measurements is estimated to be of the order of 10% (Gallet et al., 2009; Montpetit et al., 2012a), which is better than the visual estimate of D_{max} (see Langlois et al., 2010).

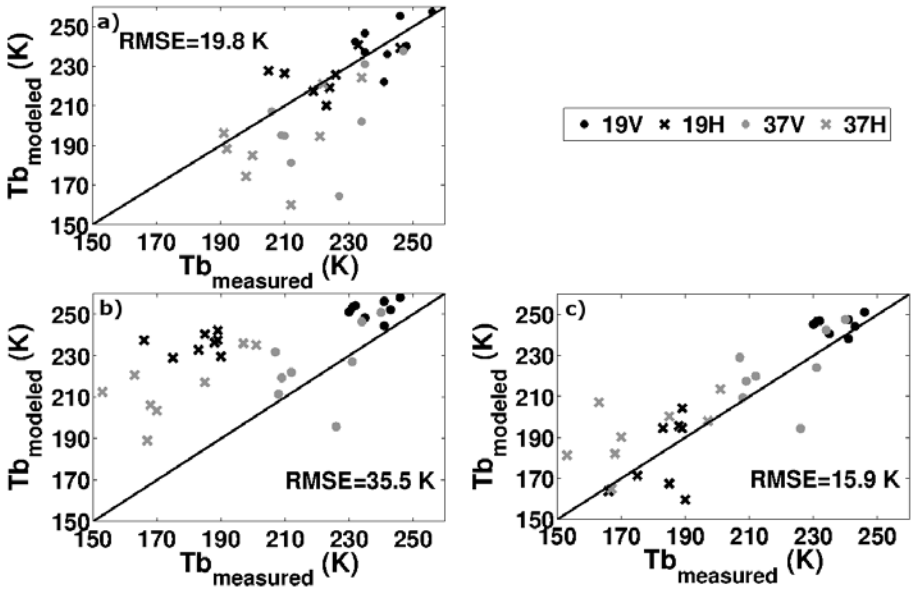

Figure 6. MEMLS was used to determine the modeled error on snow for snowpacks without any observed ice lens (a). MEMLS was used to model Tb without an ice lens (b) and with the ice lenses at their measured depths within the snowpacks (b), with $\varphi = 1.0$ and optimized $\sigma = 0.0$ cm, which were compared to measured Tb for all 8 snowpits taken at Daring Lake with ice lenses for 19 and 37 GHz and two polarizations H and V. Overall RMSE are shown.

CONCLUSIONS

The main objective of this paper was to improve the brightness temperature simulations of a snowpack having ice lenses within it and determine the sensitivity of the signal to the different properties of ice lenses. The Microwave Emission Model of Layered Snowpacks (MEMLS) was used, and an optimization process was proposed to minimize the errors due to the snow grain size measurements and to the soil reflectivity parameterization. The use of a unique and detailed dataset for the physical properties of snow allowed us to minimize the uncertainties due to snow (without ice lenses) and soil and to accurately estimate the effects of ice lenses.

The vertical location of the ice lens within the snowpack was found to be a key parameter that has to be precisely determined. This finding has important implications for operational applications of snow emission models, for instance in snow water equivalent retrieval schemes as described in Takala et al (2011). These hemispheric scale emission model implementations currently use only a single snowpack layer. To properly account for ice lenses, it would be necessary to use up to three layers: one for the lens plus an underlying snow layer and one layer above the lens if necessary. Given the lack of in situ stratigraphic snow observations at the hemispheric scale, the vertical location of ice lenses in the snowpack needs to be inferred or estimated from a physical snow model. Given the challenges in deriving multi-layer inputs for snow emission models at the hemispheric scale, stratigraphic properties such as ice lenses will likely continue to be a source of uncertainty in operational applications of snow emission models.

A multiplicative correction factor (ϕ) was applied to the snow grain size parameter derived from optical diameter measurements, and the soil parameters were fitted to improve simulations of the snow brightness temperatures at 19 and 37 GHz. The optimal factor was determined to be $\phi = 1.3$ for the snow specific surface area (SSA) measurements and $\phi = 1.0$ for snow grains defined by the longest diameter (i.e., geometrical diameter, D_{max}) measured manually. Also, a soil reflectivity ratio parameter $\beta = 1.72$ and soil roughness parameters for 2 types of sites ($\sigma_{grass} = 1.1$ cm and $\sigma_{tundra} = 0.4$ cm) were determined.

With these optimal parameters, comparisons between modeled and measured brightness temperatures were performed without the ice lens treatment, with an ice lens modeled on top of the snowpack, and with an ice lens modeled at its measured depth within the snowpack. An improvement of 13.1 K for the root mean square error was observed by modeling an ice lens on top of the snowpack and an improvement of 20.5 K when modeling the ice lenses at their measured depths within the snowpacks. The simulations presented here give an RMSE of the same order of magnitude (8–20 K) for snow without ice lenses as for snow with ice lenses.

Another comparison was conducted using an independent dataset (Rees et al., 2010) to further validate the ice lens treatment. Again, a significant improvement of 19.6 K of the RMSE was observed by modeling the ice lenses at their measured depths compared to simulations without ice lenses. The higher RMSE compared to the first dataset was explained by the snow grain size characterization that was a subjective estimate of the geometrical diameter as opposed to an objective measurement of SSA.

The next step in testing the ice lens model is to measure the ice lens density to verify if there are air bubbles within the lenses and to determine if there is any effect on the microwave signal. Also, a validation with satellite data would be useful. When validated at this scale, this model could be extremely useful in developing an algorithm to remotely detect ice lenses from satellite measurements.

ACKNOWLEDGEMENTS

The authors thank Dr. Andrew Rees and Juha Lemmetyinen for providing the Tb measurements and the MEMLS input parameters for the Daring Lake sites. All of our colleagues from France and Canada who helped us during the field campaigns are also gratefully acknowledged. The authors would also like to thank both anonymous reviewers for their contribution to the improvement of this paper. This work was supported by NSERC, the Canadian Space Agency (Canadian CoReH2O field campaign), and Environment Canada (Climate Research Division).

REFERENCES

Asmus KW, Grant C. 1999. Surface based Radiometer (SBR) data acquisition system. *International Journal of Remote Sensing* **20**: 3125–3129.

Bartsch A, Kumpula T, Forbes B, Stammler F. 2010. Detection of snow surface thawing and refreezing in the Eurasian Arctic with QuikSCAT: Implications for reindeer herding. *Ecological Applications* **20**: 2346–2358.

Brucker L, Picard G, Fily M. 2010. Snow grain-size profiles deduced from microwave snow emissivities in Antarctica. *Journal of Glaciology* **56**: 514–526.

Brucker L, Royer A, Picard G, Langlois A, Fily M. 2011. Hourly simulations of seasonal snow microwave brightness temperature using coupled snow evolution-emission models in Quebec, Canada. *Remote Sensing of Environment* **115**: 1966–1977.

Debye P, Anderson Jr. HR, Brumberger H. 1957. Scattering by an inhomogeneous solid. II. The correlation function and its application. *Journal of Applied Physics* **28**: 679–683.

Derksen C, Toose P, Lemmetyinen J, Pulliainen J, Langlois A, Rutter N, Fuller M. 2012. Evaluation of passive microwave brightness temperature simulations and snow water equivalent retrievals through a winter season. *Remote Sensing of Environment* **117**: 236–248.

Durand M, Kim E, Margulis S. 2008. Quantifying uncertainty in modeling snow microwave radiance for a mountain snowpack at the point-scale, including stratigraphic effects. *IEEE Transactions on Geoscience and Remote Sensing* **46**: 1753–1767.

Durand M, Kim E, Margulis S. 2009. Radiance assimilation shows promise for snowpack characterization. *Geophysical Research Letters* **36**.

Durand M, Liu D. 2012. The need for prior information in characterizing snow water equivalent from microwave brightness temperatures. *Remote Sensing of Environment*.

Fierz C, Armstrong R, Durand Y, Etchevers P, Greene E, McClung DM, Nishimura K, Satyawali PK, Sokratov SA. 2009. *The International Classification for Seasonal Snow on the Ground*.

IHP-VII Technical Documents in Hydrology No. 83, IACS Contribution No. 1. International Association of Cryospheric Sciences. UNESCO: Paris, France.
Gallet JC, Domine F, Zender C, and Picard G. 2009. Rapid and accurate measurements of the specific surface area of snow using infrared reflectance at 1310 and 1550 nm. *Cryosphere Discussions* **3**: 33–75.
Grenfell T, Putkonen J. 2008. A method for the detection of the severe rain-on-snow event on Banks Island, October 2003, using passive microwave remote sensing. *Water Resources Research* **44**.
Grody N. 2008. Relationship between snow parameters and microwave satellite measurements: Theory compared with Advanced Microwave Sounding Unit observations from 23 to 150 GHz. *Journal of Geophysical Research* **113**.
Hansen B, Aanes R, Herfindal I, Kohler J, Saether B,Oli M. 2011. Climate icing, and wild arctic reindeer: Past relationships and future prospects. *Ecology* **92**: 1917–1923.
Langlois A, Royer A, Derksen C, Montpetit B, Dupont F, Goita K. 2012. Coupling of the snow thermodynamic model SNOWPACK with the Microwave Emission Model for Layered Snowpacks (MEMLS) for subarctic and arctic Snow Water Equivalent retrievals. *Water Resources Research* 2012WR012133.
Langlois A, Royer A, Dupont F, Roy A, Goïta K, Picard G. 2011. Improved corrections of forest effects on passive microwave satellite remote sensing of snow over boreal and subarctic regions. *IEEE Transactions on Geoscience and Remote Sensing* **49**(10): 3824–3837.
Langlois A, Royer A, Montpetit B, Picard G, Arnaud L, Harvey-Collard P, Fily M, Goïta K. 2010. On the relationship between snow grain morphology and in-situ near infrared calibrated reflectance photographs. *Cold Regions Science and Technology* **61**: 34–42.
Lemmetyinen J, Kontu A, Rees A, Derksen C, Pulliainen J. 2010. Comparison of multiple layer snow emission models. *IEEE transactions on geosciences and remote sensing*.
Mätzler C, Wiesmann A. 1999. Extension of the microwave emission model of layered snowpacks to coarse-grained snow. *Remote Sensing of Environment* **70**: 317–325.
Mätzler C. 1998a. Improved Born approximation for scattering of radiation in a granular medium. *Journal of Applied Physics* **83**(11): 6111–6117.
Mätzler C. 1998b. Microwave Properties of Ice and Snow. In *Solar System Ices*, Schmitt B et al. (eds). Kluwer Academic Publishers: Dordrecht; 241–257.
Mätzler C. 2002. Relationship between grain-size and correlation length of snow. *Journal of Glaciology* **48**: 461–466.
Mätzler C. 2006. *Thermal microwave radiation: applications for remote sensing*. Institution of Engineering and Technology.
Miller FL, Russel RH, Gunn A. 1975. The recent decline of peary caribou on western Queen Elizabeth island of Arctic Canada. *Polarforschung* **45**: 17–21.
Montpetit B, Royer A, Langlois A, Cliche P, Roy A, Champollion N, Picard G, Domine F, and Obbard R. 2012a. New short wave infrared albedo measurements for snow specific surface area retrieval. *Journal of Glaciology* **58**: 941–952.
Montpetit B, Royer A, Roy A, Langlois A, Derksen C. 2012b. Snow microwave emission modeling of ice lenses within a snowpack using the Microwave Emission Model for Layered Snowpacks (MEMLS). *IEEE Transactions on Geoscience and Remote Sensing*, in revision.
Prigent C, Wigneron J, Rossow W, Pardo-Carrion J. 2000. Frequency and angular variations of land surface microwave emissivities: Can we estimate SSM/T and AMSU emissivities from SSM/I emissivities? *IEEE Transactions on Geoscience and Remote Sensing* **38**(5): 2373–2386.
Pulliainen JT, Grandell J, Hallikainen MT. 1999. HUT Snow Emission Model and its Applicability to Snow Water Equivalent Retrieval. *IEEE Transactions on geoscience and remote sensing* **37**: 1378–1390.
Putkonen J, Jacobson H, Rennert K. 2011. Modeled rain on snow in CLM3 warms soil under thick snow cover and cools it under thin, brief communication. *Cryosphere Discussions* **5**: 2557–2570.
Rees A, Lemmetyinen J, Derksen C, Pulliainen J, English M. 2010. Observed and modelled effects of ice lens formation on passive microwave brightness temperatures over snow covered tundra. *Remote Sensing of Environment* **114**: 116–126.

Rennert K, Roe G, Putkonen J, Bitz C. 2009. Soil thermal and ecological impacts of rain on snow events in the circumpolar arctic. *Journal of Climate* **22**: 2302–2315.
Roy A, Picard G, Royer A, Dupont F, Langlois A, Montpetit B, Derksen C. 2012. Brightness temperature simulations of the Canadian seasonal snowpack driven by measurements of the snow specific surface area. *IEEE Transactions on Geoscience and Remote Sensing*, in revision.
Serreze M, Barry R. 2011. Processes and impacts of Arctic amplification: A research synthesis. *Global and Planetary Change* **B**: 85–96.
Solheim F. 1993. *Use of pointed water vapor radiometers to improve GPS surveying accuracy*. Ph.D. dissertation. University of Colorado: Boulder, CO.
Stien A, Loel L, Mysterud A, Severinsen T, Kohler J, Langvatn R. 2010. Icing events trigger range displacement in a high-arctic ungulate. *Ecology* **91**: 915–920.
Takala M, Luojus K, Pulliainen J, Derksen C, Lemmetyinen J, Kärnä J-P, KoskinenJ. 2011. Estimating northern hemisphere snow water equivalent for climate research through assimilation of space-borne radiometer data and ground-based measurements. *Remote Sensing of Environment* **115**(12): 3517–3529. doi:10.1016/j.rse.2011.08.014.
Wegmüller U, Mätzler C. 1999. Rough bare soil reflectivity model. *IEEE Transactions on Geoscience and Remote Sensing* **37**(3): 1391–1395.
Wiesmann A, Fierz C, Mätzler C. 2000. Simulation of microwave emission from physically modeled snowpacks. *Annals of Glaciology* **31**: 397–401.
Wiesmann A, Mätzler C. 1999. Microwave Emission Model of Layered Snowpacks. *Remote Sensing of Environment* **70**: 307–316.
Wigneron J, Chanzy A, Kerr Y, Lawrence H, Shi J, Escorihuela M, Mironov V, Mialon A, Demontoux F, De Rosnay P, Saleh-Contell K. 2011. Evaluating an improved parameterization of the soil emission in L-MEB. *IEEE Transactions on Geoscience and Remote Sensing* **49**: 1177–1189.
Ye H, Yang D, Robinson D. 2008. Winter rain on snow and its association with air temperature in northern Eurasia. *Hydrological Processes* **22**: 2728–2736.